

Development of a controller to perform an automatic lateral emergency collision avoidance manoeuvre for a passenger car

Geraint Bevan, Henrik Gollee and John O'Reilly

Centre for Systems and Control

University of Glasgow, GLASGOW. G12 8QQ Scotland.

+44 (0)141 330 T: 4723 F: 4343 g.bevan@eng.gla.ac.uk

March 21, 2006

Abstract

An automatic controller is being developed to cause a passenger car to perform a lateral emergency collision avoidance manoeuvre: a single lane change at high speed, while operating at the vehicle's physical limits.

The car is stabilised about a predetermined velocity profile by a feedforward steering action based on the Ackermann steering angle, combined with a feedback control loop which uses the anti-lock braking system to apply differential torques to each of the wheels. The forces to be applied to each wheel are calculated using the pseudo-inverse of a velocity-based linearisation of a system model.

This inverse controller acts upon a signal containing the lateral and yaw velocity error, fed back through a scheduled gain matrix; the matrix, obtained by pole placement and scheduled according to the vehicle state, causes the car to exhibit uniform dynamic behaviour as its speed increases.

An additional control loop augments the steering angle of the front wheels, using actuators which form part of a steer-by-wire system, to correct for errors in the lateral position and heading angle for which the force/velocity control loop does not account.

The control system is evaluated in simulation experiments which show that the performance requirements are met over a wide range of velocities.

Introduction

As roads become busier and technology improves, there is a growing potential for driver assistance systems to improve the safety of road users. It is becoming increasingly common for luxury cars to be fitted with longitudinal collision avoidance systems, where cruise control functions are integrated with forward looking obstacle detection sensors to automatically slow the car when necessary.

Such devices can be a valuable aid if an impending rear-end collision between cars travelling in the same lane is due to driver inattention and the vehicles are amply separated in space and time for the aft vehicle to brake. They are, however, of limited benefit for preventing head-on collisions or avoiding obstacles which appear suddenly in front of a moving vehicle. In these circumstances, aggressive lateral manoeuvres are more appropriate; as well as altering the path of the vehicle to move it out of danger, the manoeuvre can be completed in a shorter distance than that required to bring the vehicle to a stop.

The availability of steer-by-wire augmentation and electronic stability programmes can enable such manoeuvres to be initiated and performed under the guidance of a vehicle management computer. One of the aims of the CEMACS project is to produce such a controller which will cause a car to change lanes while operating at its physical limits. There are clearly many technologies that must come together to bring such a system to fruition on production vehicles - particularly with regard to situational awareness - as well as legal issues that must be considered, but these issues are beyond the scope of the CEMACS project.

Vehicle design model

The development of an appropriate linear model, or family of models, is an important part of conventional controller design. During an aggressive lane change manoeuvre the vehicle is expected to operate far from equilibrium conditions and with potentially large and fast changing control inputs.

Non-linear model

A two track non-linear model of a vehicle was developed, with three vehicle body states and five control inputs. This non-linear model is of the form $\dot{\mathbf{x}} = \mathcal{F}(\mathbf{x}, \mathbf{u})$ where the state and input vectors are defined as $\mathbf{x} = (X, Y, \Psi)^T$ and $\mathbf{u} = (\mathbf{f}_X, \delta)^T$. The state vector \mathbf{x} comprises of the vehicle longitudinal position, X ; lateral position, Y ; and yaw angle, Ψ . The input vector \mathbf{u} comprises of the longitudinal forces on each of the four wheels, \mathbf{f}_X ; and the steering angle of the front wheels, δ .

Velocity based linearisation

The velocity based method of Leith and Leithead [1998] enables linearisations of models to be obtained under non-equilibrium conditions and is not constrained by the restriction to small inputs that can arise from conventional small perturbation linearisation. The suitability of the method has been demonstrated for other vehicle dynamics problems which demand high performance [Leith et al., 2001].

Differentiating the non-linear model with respect to time t results in a family of linear models defined by a scheduling vector $\rho = (\mathbf{x}, \mathbf{u})^T$:

$$\ddot{\mathbf{x}} = \mathbf{A}(\rho)\dot{\mathbf{x}} + \mathbf{B}(\rho)\dot{\mathbf{u}}$$

where $\mathbf{A}(\rho) = \frac{\partial \mathcal{F}}{\partial \mathbf{x}}$ and $\mathbf{B}(\rho) = \frac{\partial \mathcal{F}}{\partial \mathbf{u}}$.

For this particular model, the longitudinal wheel forces do not appear in the state and input matrices of the linearised model so the scheduling parameter can be reduced to $\rho = (\mathbf{x}, \delta)^T$.

Implementation

The non-linear model was implemented in C++ and wrappers were written to enable it to be dynamically loaded and called from the Matlab and GNU Octave matrix algebra tools. Functions were created to calculate the velocity-linearised state and input matrices for any operating condition. The A and B matrices can therefore be used for linear controller design, while the non-linear model can be used to perform a basic evaluation of performance by simulation.

Controller architecture

There are three distinct elements to the controller architecture shown in figure 1.

The simplest is a feedforward controller $\mathcal{D}(x_{ref})$ which assigns a nominal steering angle δ_0 on the basis of a predetermined profile, scheduled according to the longitudinal position of the vehicle relative to its reference trajectory. This reference steering profile is derived from the Ackermann steering angle, i.e. the geometrically-derived angle which would cause the vehicle to follow the path in the absence of slip. However, there is nothing particularly special about this profile and any suitable alternative could be substituted without impacting the controller architecture.

Two parallel loops provide stabilisation about the reference trajectory. A velocity loop, shown in blue, controls the vehicle lateral and yaw velocity (Y and $\dot{\Psi}$) by altering the longitudinal tyre forces, using the ABS slip controller. A position loop, shown in red, controls the lateral position of the vehicle by augmenting the steering angle of the front wheels with an additional steering input Δ .

Force/Velocity loop

The force/velocity loop consists of a scheduled gain matrix $L(\rho)$ and a pseudo-inverse B_f^{-1} of that part of the linearised input matrix that relates to vehicle forces.

L is designed to give the vehicle uniform dynamic behaviour as its operating condition changes. The open-loop poles of the plant were identified from the model when the car was driven at low speed. Pole placement was then used to force the poles to remain at these locations as the velocity changes. The behaviour of the closed loop is approximately

$$\frac{\dot{\theta}}{\dot{\theta}_{\text{ref}}} \approx \frac{1}{s(s + 0.015)(s + 0.03)}$$

where $\dot{\theta} = (\dot{Y}, \dot{\Psi})^T$.

It is not necessary to explicitly control the longitudinal velocity of the vehicle and attempting to do so would reduce the available traction which can be used for providing lateral acceleration. The reference longitudinal velocity is therefore set to be equal to the measured velocity, effectively setting the error in this signal to zero.

Steering/Position loop

The feedforward C_f and feedback C_b controllers of the position loop eliminate the steady state error that would result if the velocity loop existed in isolation. They were designed by direct synthesis, using an approximation to the vehicle's dynamic behaviour. The approximation was obtained by averaging the frequency response of the car over a range of conditions. The closed loop specification was chosen to be of the form

$$\frac{Y}{Y_{\text{ref}}} = \frac{K \frac{\omega^2}{\tau}}{(s + \frac{1}{\tau})(s^2 + 2\zeta\omega s + \omega^2)}$$

Sensitivity and robustness

The controller L does not attempt to control the forward velocity \dot{X} so only the sensitivity and robustness of the channels with lateral and yaw velocity outputs need be considered.

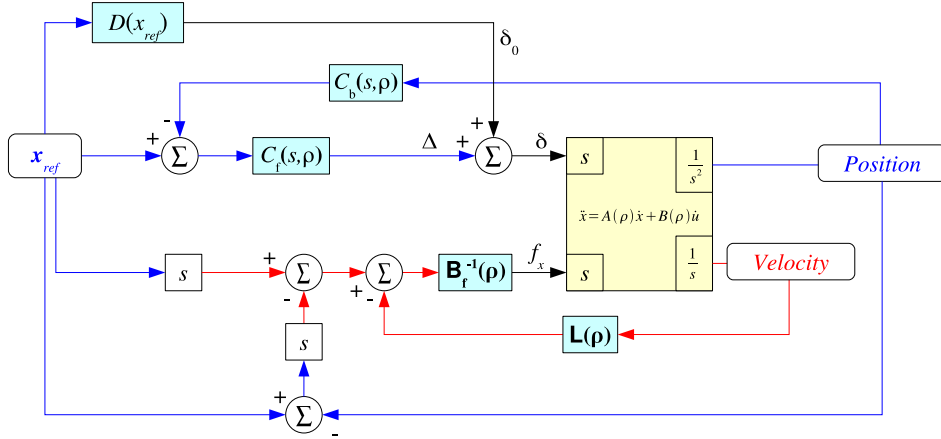


Figure 1: Controller architecture: A feedforward controller (D) provides a pre-determined nominal steering angle to coerce the car to follow its target trajectory. A lateral position control loop augments the nominal steering angle using feedforward and feedback controllers C_f and C_b . In parallel, a force/velocity loop consisting of a scheduled gain matrix L and pseudo-inverse B_f^{-1} of the linearised input matrix stabilises the car about its reference velocity profile and provides uniform dynamics as the velocity changes.

Disturbance rejection

Sensitivity functions $S(i\omega)$ for the channels with lateral and yaw velocity outputs are shown in figure 2. It can be seen that both of these outputs are entirely insensitive to disturbances in the vehicle longitudinal velocity at all frequencies.

It should be noted here that the nominal plant changes with the speed of the vehicle and that this does not therefore provide any guarantee that the model will perform well at velocities far removed from 80 kph but does provide some confidence that the system will cope reasonably well with minor speed changes during the course of the manoeuvre.

The lateral velocity ceases to reject disturbances to itself at fairly low frequencies. This channel is seen to have a bandwidth varying from approximately 5×10^{-3} radians per second with the wheels pointing straight ahead, increasing

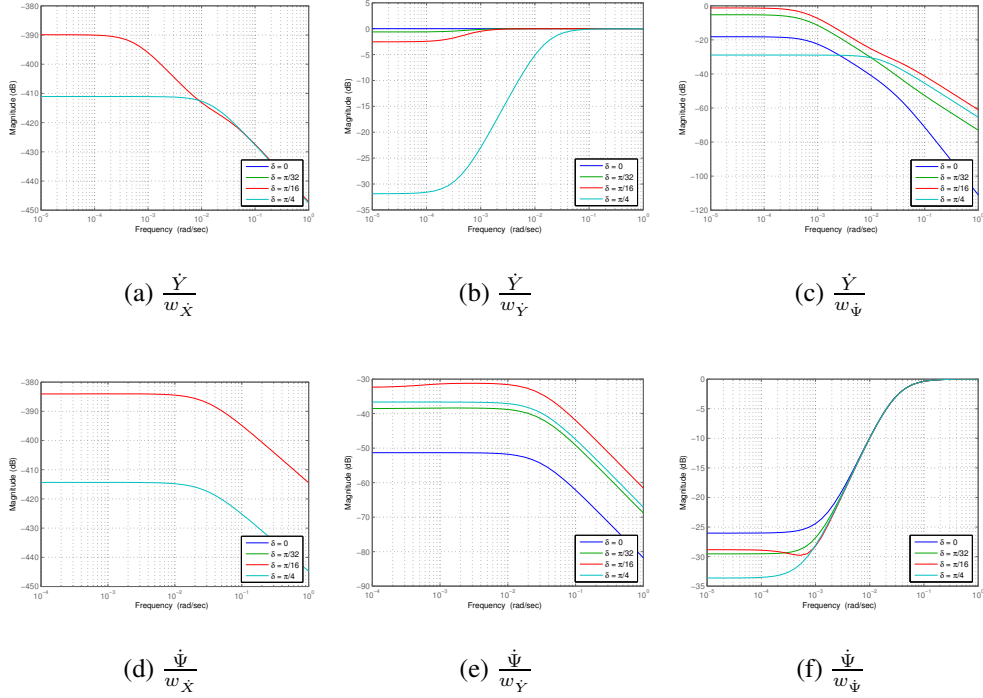


Figure 2: Sensitivity functions, showing the response of the lateral and yaw velocities of the nominal system to disturbances in the states at a forward speed of 80 kph for four steering angles δ .

by an order of magnitude to 5×10^{-2} radians per second as the front wheels are turned to a steering angle of $\frac{\pi}{4}$ radians.

Disturbances in the yaw velocity are rejected by the lateral velocity at all frequencies, with very low sensitivity at frequencies higher than approximately 10^{-3} radians per second for all steering angles.

The yaw velocity rejects disturbances on all input channels, with little sensitivity to longitudinal and lateral velocity disturbances and very low sensitivity to yaw rate disturbances above 10^{-2} radians per second

Sensitivity to model errors

Assuming that the uncertainty in the vehicle model can be characterised as $G = \bar{G}(I + \Delta_G)$ where \bar{G} is the nominal model and Δ_G the model uncertainty at the output, the system will be robust to model uncertainties if the complementary sensitivity T and uncertainty satisfy $|T(i\omega)\Delta_G(i\omega)| < 1 \quad \forall \omega$.

Complementary sensitivity functions are shown for the in figure 3 for the chan-

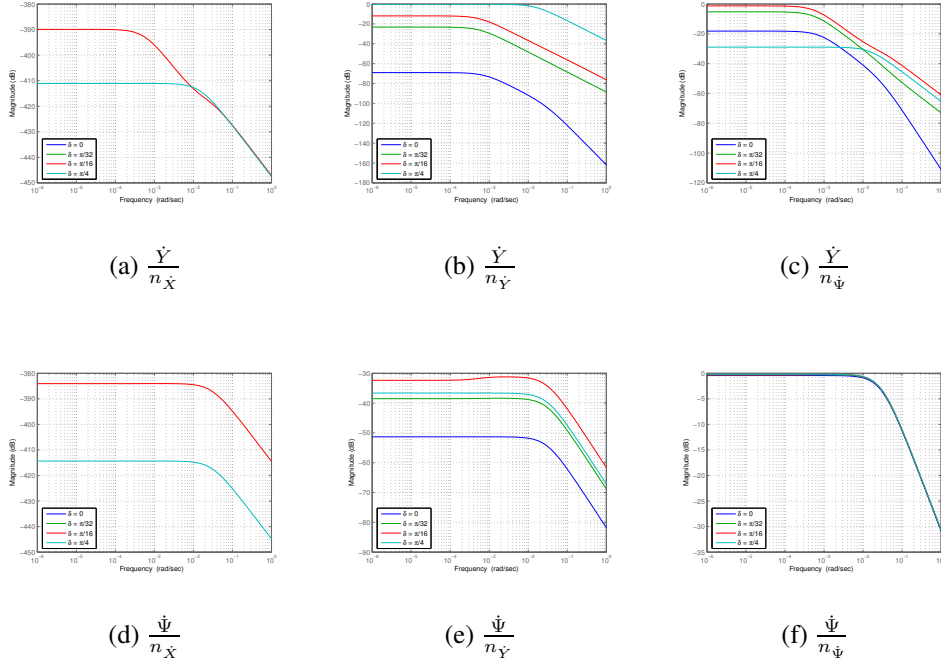


Figure 3: Complementary sensitivity functions, showing the response of the lateral and yaw velocities of the nominal system to noise in the output signals at a forward speed of 80 kph for four steering angles δ .

nels with lateral and yaw velocity outputs.

The maximum sensitivities to uncertainty on any of the six channels that output lateral or yaw velocity are of magnitude one, occurring on the channels linking lateral velocity noise to lateral velocity output, and yaw rate noise to yaw rate output. In both of these cases, the sensitivity to noise rolls off significantly as its frequency increases.

Specification

The lane change manoeuvre to be performed was adapted from the ISO standard for severe lane change manoeuvres ISO [2002].

The lane change manoeuvre is to be conducted as quickly as possible, taking the vehicle to its physical limits.

Five control inputs are available to manoeuvre the vehicle: front wheel steering and control of the longitudinal forces on each wheel, through the anti-lock braking system (ABS). Actuator constraints were provided by the vehicle manu-

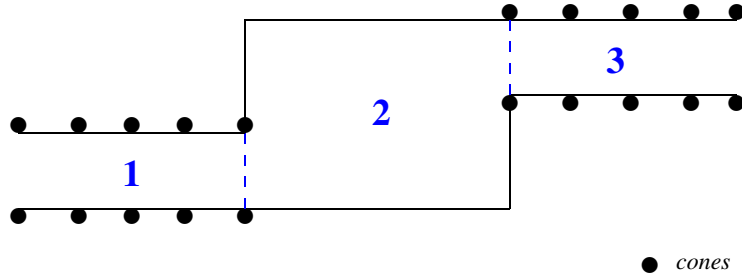


Figure 4: Test track layout for demonstration of severe lane change derived from ISO 3888-2:2002 *Passenger cars – Test track for a severe lane-change manoeuvre – Part 2: Obstacle avoidance*

| Section | Length (metres) | Width (metres) |
|---------|-----------------|--|
| 1 | 12.0 | $1.1 \times \text{vehicle width} + 0.25$ |
| 2 | 13.5 | $2.1 \times \text{vehicle width} + 1.25$ |
| 3 | 11.0 | $1.0 \times \text{vehicle width} + 1.00$ |

Table 1: Test track dimensions

facturer.

For the purposes of this controller, it is assumed that the vehicle position, velocity and acceleration are well known and available from the vehicle management computer.

Taking into account the width of the car, a step change of 2.26 metres would allow a margin of 0.55 metres either side of the centre line as the car moves into the final section (3 on the diagram), corresponding to a maximum overshoot/undershoot of approximately 24%.

A suitable reference trajectory to manoeuvre the car through the test sections can be defined by the function:

$$Y_0(X) = \begin{cases} 0 & (0.0 \leq X < 12.0) \\ 1.13 \times \left(1 + \sin\left(\pi \frac{X-12.0}{1.5} - \frac{\pi}{2}\right)\right) & (12.0 \leq X < 25.5) \\ 2.26 & (25.5 \leq X) \end{cases}$$

which provides a margin of approximately four metres in the X direction between the reference trajectory and the first cone at the start of the final section. Consequently, the vehicle must not lag the reference trajectory by a time greater than $\frac{4}{X}$ seconds.

Simulation results

The results of simulations using the non-linear vehicle model are shown in figures 5 to 8 for four speeds: 80, 60, 40 and 20 kph. In each case, the vehicle started with the given longitudinal speed and zero lateral and yaw velocity.

Subfigure (a) in each figure shows the feedforward steering angle (δ_0 , shown in blue) and the combined steering angle ($\delta = \delta_0 + \Delta$, shown in green) that results from the action of the steering/position loop. The steering controller was designed to operate at speeds of about 80 kph so there is some poor performance at very low speeds, as is evident in the oscillatory behaviour seen in figure 8.

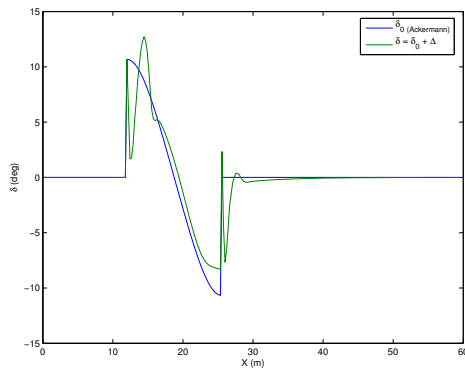
Subfigure (b) shows the reference (blue) and actual (green) yaw angle as the car performs the manoeuvre.

Subfigure (c) shows the longitudinal forces that act on each wheel. These forces are the output of the inverse model \mathcal{D} , acting upon the error signals that result from the gain matrix L . It can be seen that in each case the wheels on opposite sides of the vehicle act in opposite directions as the controller stabilises the yaw rate. As expected, the output of the force controller decreases as the vehicle velocity decreases.

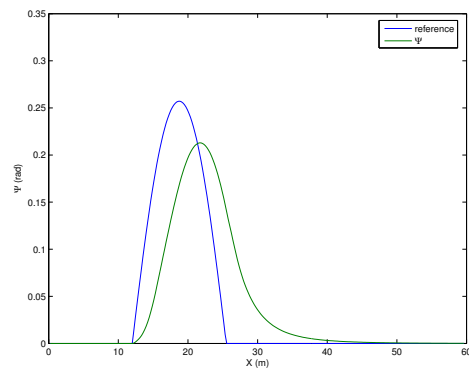
Subfigure (d) shows the trajectory taken by the vehicle. The coloured dashed lines depict the boundary of the manoeuvre area while the dotted black lines show the approximate limits for the vehicle centre of gravity if the side of the car is not to exceed the coned boundary. The blue solid line shows the reference trajectory while the green line shows the path taken by the vehicle. In all cases, the vehicle stays within the limits and completes the manoeuvre successfully.

References

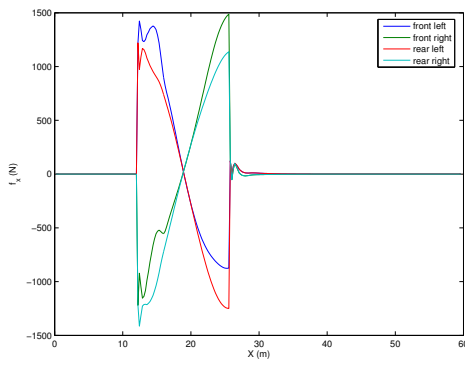
- ISO-3888-2:2002 passenger cars - test track for a severe lane-change manoeuvre – part 2: Obstacle avoidance, 2002.
- D. J. Leith and W. E. Leithead. Gain-scheduled and nonlinear systems: dynamic analysis by velocity-based linearization families. *International Journal of Control*, 70(2):289–317, May 1998.
- D.J. Leith, A. Tsourdos, B.A. White, and W.E. Leithead. Application of velocity-based gain-scheduling to lateral auto-pilot design for an agile missile. *Control Engineering Practice*, 9(10):1079 – 1093, 2001. ISSN 0967-0661. URL [http://dx.doi.org/10.1016/S0967-0661\(01\)00077-6](http://dx.doi.org/10.1016/S0967-0661(01)00077-6). Auto pilot design;.



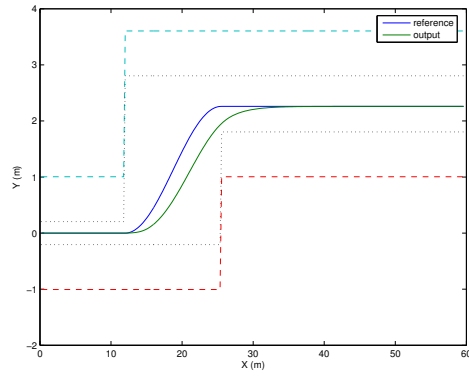
(a) Steering angle



(b) Yaw angle

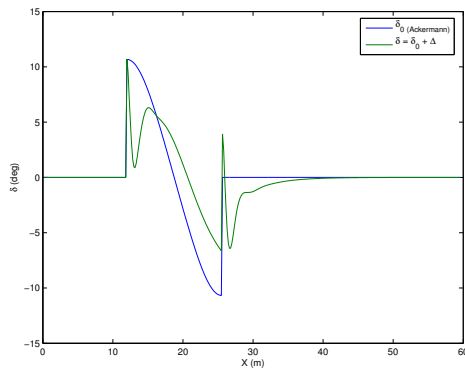


(c) Tyre forces

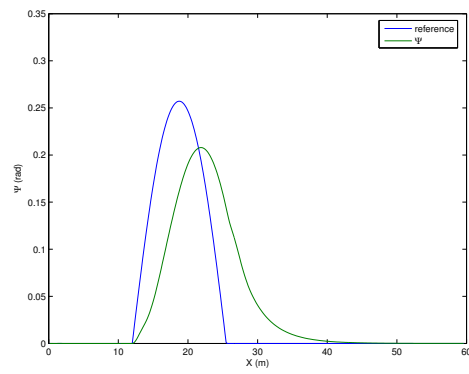


(d) Trajectory

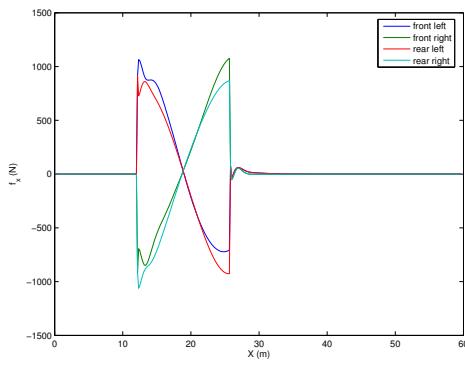
Figure 5: Simulation results at 80 kph



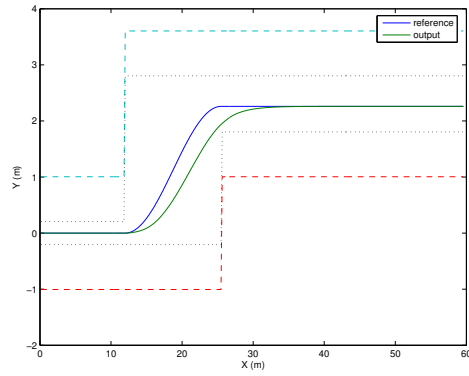
(a) Steering angle



(b) Yaw angle

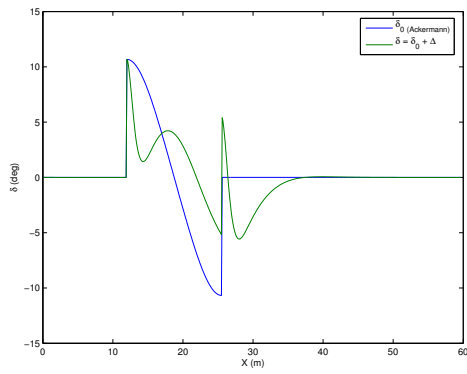


(c) Tyre forces

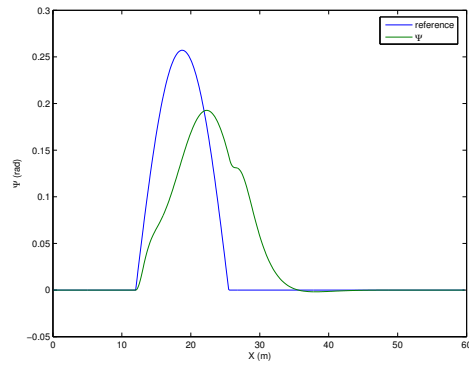


(d) Trajectory

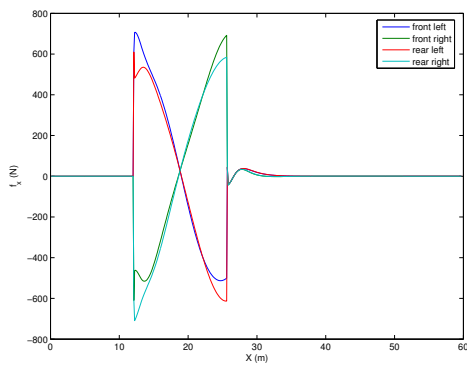
Figure 6: Simulation results at 60 kph



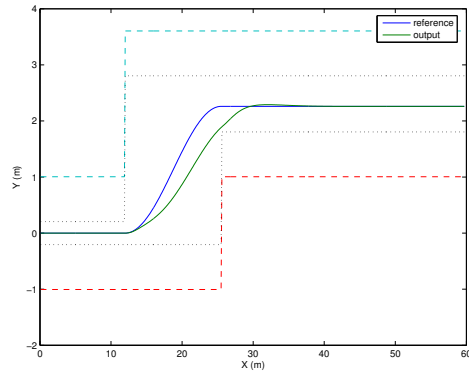
(a) Steering angle



(b) Yaw angle

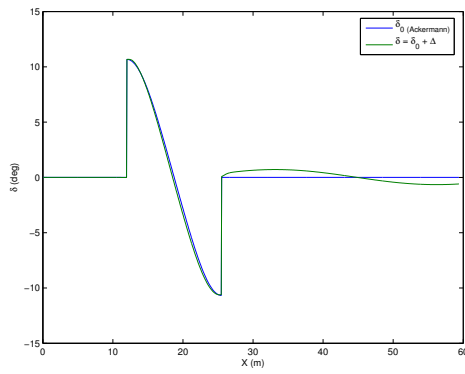


(c) Tyre forces

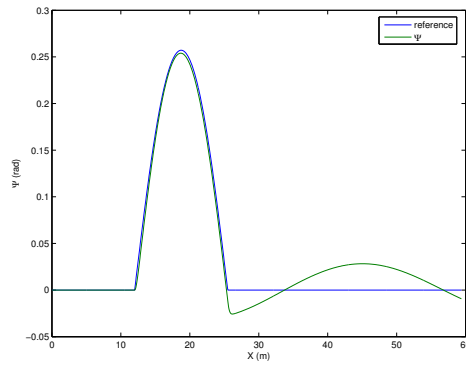


(d) Trajectory

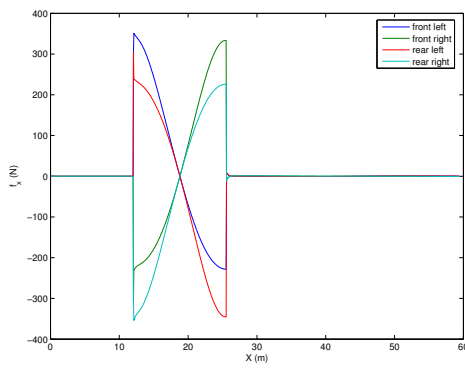
Figure 7: Simulation results at 40 kph



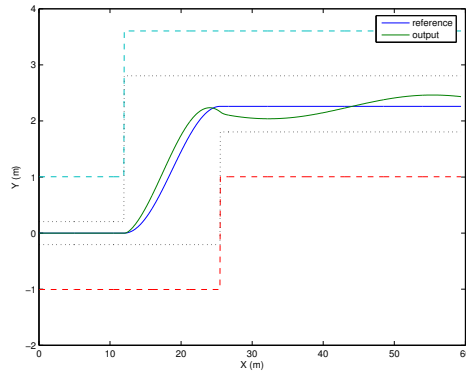
(a) Steering angle



(b) Yaw angle



(c) Tyre forces



(d) Trajectory

Figure 8: Simulation results at 20 kph